New Diamond and Frontier Carbon Technology
Vol. 16, No. 1 2006
MYU Tokyo

NDFCT 503

Anticoagulation Behavior of Phosphorus-Doped Carbon (P_xC) Films Synthesized by Plasma Immersion Ion Implantation and Deposition

Sunny C. H. Kwok[1,2], Guojiang Wan[1,3], Joan P. Y. Ho[1,2], Paul K. Chu[1,*], David R. McKenzie[2], Marcela M. M. Bilek[2]

[1]Department of Physics and Materials Science, City University of Hong Kong, Tat Chee Avenue, Kowloon, Hong Kong (SAR)
[2]Applied and Plasma Physics Group, School of Physics, A28, University of Sydney, NSW 2006, Australia
[3]School of Materials Science and Engineering, Southwest Jiaotong University, Chengdu 610031, China

(Received 14 October 2005; accepted 21 February 2006)

Key words: phosphorus-doped carbon (P_xC) films, anticoagulation, wettability, plasma immersion ion implantation and deposition (PIII&D)

In our previous work, we demonstrated that diamond-like carbon (DLC) or amorphous carbon (a-C) films doped with phosphorus exhibited improved surface blood compatibility. In this work, DLC films with different phosphorus contents (P_xC) were synthesized by plasma immersion ion implantation and deposition (PIII&D) to investigate the effects of the concentrations of phosphorus as well as the enhancement mechanism. On the basis of the results of film characterization, surface energy analysis and platelet adhesion tests, good compatibility behavior occurs on the sample with a particular concentration of phosphorus. The proper amount of dopant yields a higher surface interfacial energy for albumin but a lower one for fibrinogen, resulting in low platelet adhesion and activation. Our results suggest that the biocompatibility improvement observed on the P_xC film stems from the surface energy change that is dictated by the amount of phosphorus in the film. P_xC films with the proper phosphorus content exhibit good anticoagulation characteristics, which make them suitable as coatings in cardiovascular implantable devices such as stents and artificial heart valves.

*Corresponding author: e-mail: paul.chu@cityu.edu.hk

1. Introduction

Diamond-like carbon is known for its superior chemical, mechanical and biological properties and these properties can be enhanced by the addition of other elements within a certain concentration range. Doped carbon or diamond-like carbon (DLC) films[1] have attracted much attention recently as potential semiconducting materials. By incorporating different elements, the band gap of the materials can be altered. For instance, p-type and n-type carbon films have been fabricated by doping with boron[2] and nitrogen,[3,4] respectively. The recently discovered n-type behavior in phosphorus-doped carbon (P-C) films has spurred much research by semiconductor and materials scientists.[5–8] At the same time, doped carbon films are potentially useful biomaterials. The study of phosphorus-doped DLC in biomedical applications has, however, been limited.[9] In our previous study,[10] it was found that P-doped C films exhibited better blood compatibility than low-temperature isotropic carbon (LTIC), which is a common material in blood-contacting biomedical devices. Our further investigation reveals that the materials possess excellent wettability. This appears to be one of the reasons for the good hemocompatibility brought about by minimizing the interactions with plasma proteins, thereby resulting in slight conformational changes in absorbed plasma proteins and preferentially absorbed albumin. In this paper, we report our findings on the dependence of the enhancement effects on the phosphorus doping concentrations as well as the possible cause for the enhancement.

2. Experimental Details

2.1 *Film preparation*

A series of carbon films with different P concentrations, designated as P_xC films, were synthesized by plasma immersion ion implantation and deposition (PIII&D).[11] The amorphous carbon films were fabricated using acetylene (C_2H_2) with argon as the carrier gas. A small container with 99.9% pure red phosphorus powders was placed in the chamber as shown in Fig. 1 to produce phosphorus vapor via evaporation when heated by a filament. The mixed gases were ignited by a 500 W radio frequency (RF) source to produce the plasma in the chamber.

Si (100) substrates were used and they were cleaned by argon sputtering for 15 min prior to film deposition. By changing the experimental parameters such as the gas flow ratios of C_2H_2 to Ar, pulsed substrate bias voltages, as well as the filament current of the phosphorus source, DLC films with different P concentrations were deposited. The typical deposition time was 60 min and the experimental parameters are shown in Table 1.

2.2 *Film characterization*

Scanning electron microscopy (SEM) was used to observe the surface morphology and cross-sectional transmission electron microscopy (X-TEM) was utilized to study the microstructures of the P_xC films. Elemental mapping and chemical composition analysis were conducted using scanning electron microscopy – electron dispersive spectrometry (SEM-EDS) and X-ray photoelectron spectroscopy (XPS), respectively.

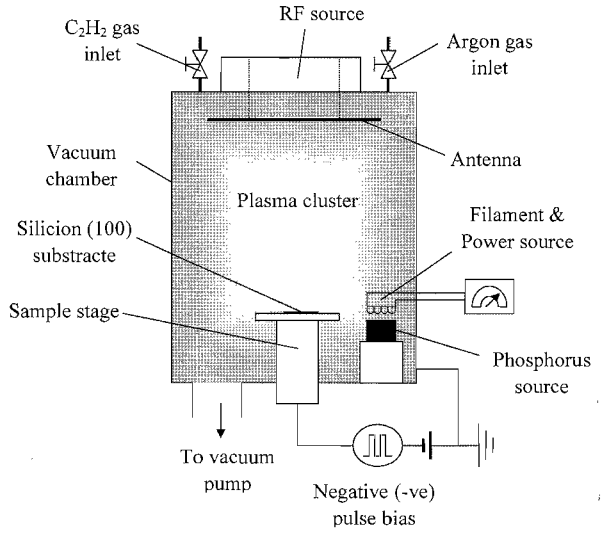

Fig. 1. Plasma immersion ion implantation (PIII&D) instrumental setup.

Table 1
Experimental parameters.

Sample	Ar/C_2H_2 (sccm)	Bias voltage (kV)	Bias frequency (Hz)/ pulse length (μs)	Filament power (W)
Sample a	8/4	−15	100/100	42
Sample b	10/10	−30	100/100	42
Sample c	10/10	−15	100/100	42
Sample d	10/10	−15	100/100	16

2.3 *Blood compatibility* – in vitro *platelet adhesion test*

Surface biocompatibility was assessed utilizing conventional *in vitro* platelet adhesion tests. The samples were incubated in a fresh human platelet-rich plasma (PRP) at 37°C for 20 min. After rinsing, fixing, and critical-point drying, the quantity and morphology of the adherent platelets were examined using optical microscopy and scanning electron microscopy (SEM). Six fields of view were chosen randomly in order to obtain good statistical results.

2.4 *Contact angle measurement and surface energy calculation*

Surface wettability was determined by the sessile drop technique using a JY-82 contact angle goniometer. Five testing fluids, namely, water, glycol, tritolyl phosphate, formamide, and diiodomethane, were used in our tests, and each test was conducted six times on different locations to obtain statistical averages. The interfacial tension between two condensed phases can be determined by the Young equation (eq. (1))[12] and Van Oss equation (eq. (2)):[13]

$$W_a = \gamma_l(1+\cos\theta) \tag{1}$$

$$W_a = 2\sqrt{\gamma_l^p \gamma_s^p} + 2\sqrt{\gamma_l^d \gamma_s^d} \tag{2}$$

where W_a is the work of adhesion, θ is the contact angle, γ_l^p and γ_l^d are the polar and dispersive components of the surface tension of the liquid phases, respectively, and γ_s^p and γ_s^d are the polar and dispersive components of the surface tension of the solid phases, respectively. We can obtain the following equation from eqs. (1) and (2):

$$\gamma_l(1+\cos\theta) = 2\sqrt{\gamma_l^p \gamma_s^p} + 2\sqrt{\gamma_l^d \gamma_s^d}\,. \tag{3}$$

By measuring the contact angles of any two different testing fluids with known polar and dispersive components (Table 2), eq. (3) can be solved to determine the polar and dispersive components of the materials.

3. Results and Discussion

3.1 *Platelet adhesion and activation*

The platelet adhesion test is one of the common and simple *in vitro* methods of evaluating blood-contacting biomaterials. The quantity and morphological change of the adherent platelets provide qualitative information on the behavior of platelets on the material surfaces. The size of the unactivated (good) platelets is typically about 2–3 μm and they maintain a disk shape. Slight pseudopodia indicate the early stage of activation, while more extensive pseudopodia and sizes > 5 μm represent a high degree of activation.

Typical SEM photos revealing the quantity and state of the adherent platelets on the different P_xC films and low-temperature isotropic carbon (LTIC) are exhibited in Fig. 2, and the statistical results are displayed in Table 3 and Fig. 3. From the perspective of the quantity of adherent platelets, all P_xC samples except sample b (Fig. 2(b)) have more adherent platelets than LTIC, but the number of good adherent platelets on samples c and d (Figs. 2(c) and 2(d)) is higher than that on LTIC. The spreading states of pseudopodia are also smaller than that on LTIC. Sample b has the smallest number of adherent platelets. In addition, the platelets are isolated and nearly round, exhibiting merely slight pseudopodia.

Table 2
Surface tension and surface tension components (dispersive and polar) of different testing liquids used in contact angle tests.

Liquid	γ(mJ/m^2)	γ_l^d (mJ/m^2)	γ_l^p (mJ/m^2)
Water	72.8	21.8	51.0
Glycol	48.3	29.3	19
Tritolyl phosphate	40.9	39.2	1.7
Formamide	58.2	39.5	18.7
Diiodomethane	50.8	48.5	2.3

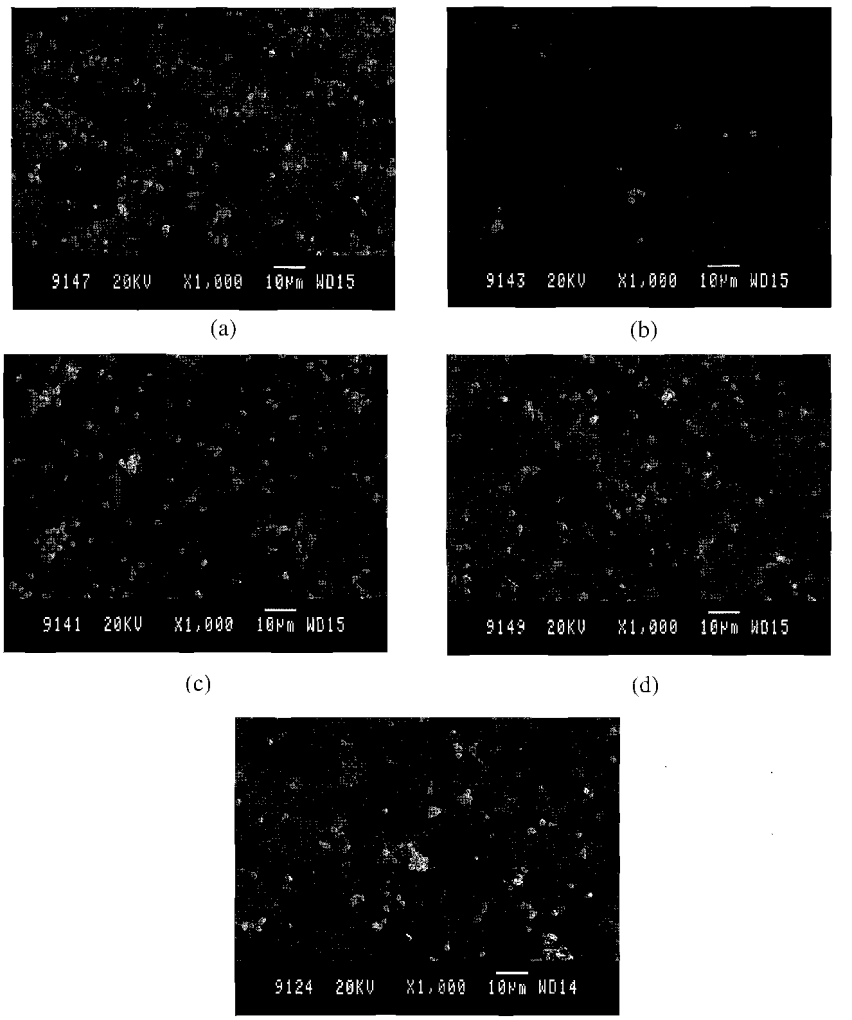

Fig. 2. SEM photos indicating platelet adhesion on samples a to d (Table 1) as well LTIC as control.

Table 3
Statistical results derived from platelet adhesion tests.

Sample	Total no. of adhesive platelets	Total no. of good platelets
P-C (a)	211	5
P-C (b)	16	14
P-C (c)	139	70
P-C (d)	140	60
LTIC	99	23

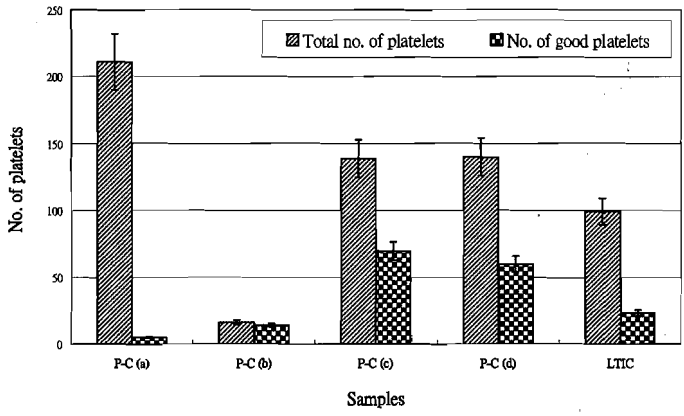

Fig. 3. Platelet adhesion test results.

3.2 *Film structure and composition*

The P_xC films are amorphous as confirmed by electron diffraction analysis in our TEM investigation (not shown). The thickness of the films is about 70 to 100 nm. A cross-sectional TEM image of sample b is shown in Fig. 4. The black dots along the interface between the film and the Si substrate are damages caused by ion implantation. Figure 5 shows the elemental map across sample b acquired using SEM-EDS (images were acquired from the same area shown in Fig. 4), showing that the carbon and phosphorus concentrations are uniform laterally (the silicon signals originate from the substrate).

The chemical composition and dopant (phosphorus) concentration were studied using XPS. The survey spectrum of sample b is shown in Fig. 6(a). Figures 6(b), 6(c) and 6(d) show the peaks of C1s (~ 284 eV), P2s (~ 192 eV) and P2p (~ 130 eV), respectively. Similar C, P, and Si spectra were also obtained from the other samples. The results reveal that P has been successfully incorporated into the carbon matrix. The slight peak shifts indicate the different dopant concentration as well as the chemical bonds between the carbon and phosphorus atoms in the films.

Figure 7 shows the P to C ratios determined from the samples. The atomic percentage of P incorporated into the film is related to the experimental parameters described in Table 1. Sample b, which fares the best in our platelet adhesion test, has a ratio of 0.27.

3.3 *Surface energy and wettability*

Surface energy measurements were conducted because surface energy is one of the crucial factors for explaining the relationship between blood compatibility and surface properties of the films. When blood comes in contact with a foreign material, plasma proteins (albumin and fibrinogen) adsorb onto the surface. The degree of platelet adhesion depends on the amount and degree of conformational changes of the adsorbed proteins. It is well known that albumin is a platelet-adhesion-inhibiting protein,[14] whereas fibrinogen is a platelet-adhesion-promoting and -activating protein.[15] The activated adherent platelets

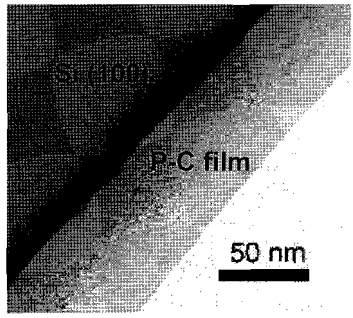

Fig. 4. X-TEM micrograph of sample b.

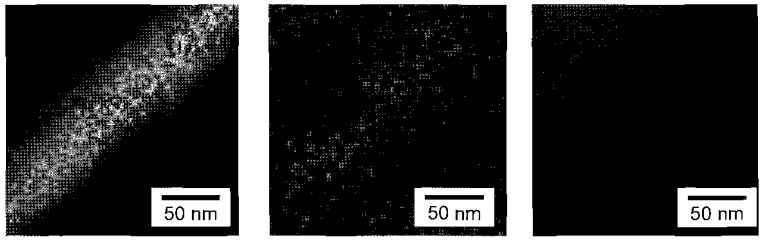

Fig. 5. Lateral elemental maps across sample b acquired using SEM-EDS.

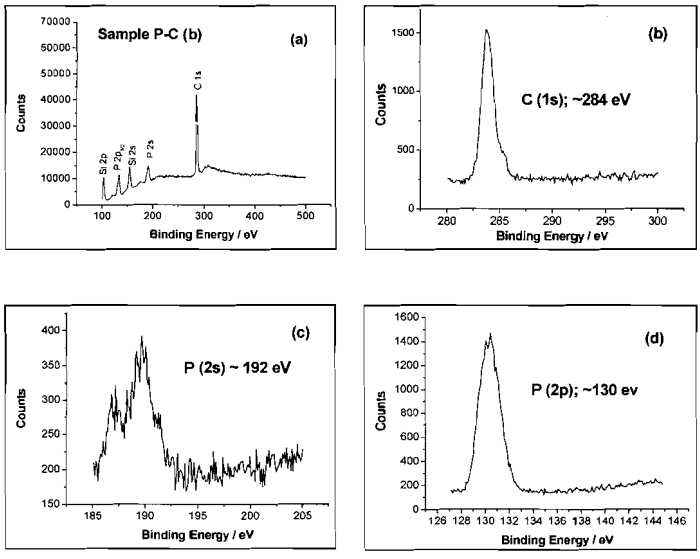

Fig. 6. XPS results of sample b. (a) Survey spectrum, (b) C1s, (c) P2s and (d) P2p spectra.

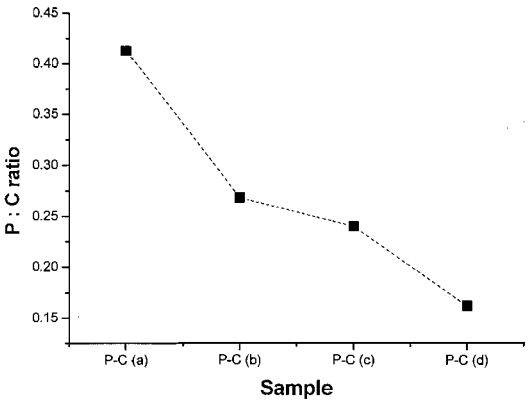

Fig. 7. P:C ratios determined by X-ray photoelectron spectroscopy (XPS).

will release certain chemical substances, provoking the adhesion of white blood cells and red blood cells on the adsorbed protein layer (with adherent platelets) and eventually causing blood coagulation or thrombus.[16] Liu *et al.* [17] reported that surface adsorption of different plasma proteins would influence the hemocompatibitlity of materials. They conducted a series of blood contact tests on polyacrylonitrile (PAN) samples which were immobilized with human serum albumin, collagen, or heparin. The study demonstrated that a sample with absorbed albumin was capable of improving the hemocompatiblity. Yang *et al.*[18] also claimed that the higher value of work of adhesion (W_a) of albumin than fibrinogen would reduce the adhesion and activation of platelets on the materials. Thus, when estimating the hemocompatibility of biomaterials, we should consider the surface energy of the materials, especially the interfacial energy between different proteins and materials.

According to Sharma,[19] the magnitude of the polar/dispersive ratio indicates the adhesion strength and level of conformational changes of plasma proteins on a material. Table 4 shows the interfacial energy (γ_{sp}) between different materials and plasma proteins (calculation details can be found in ref. 10). It can be observed that sample b has the lowest value (0.11) of $\gamma_{sp}^{p}/\gamma_{sp}^{d}$ for albumin (γ_{sp}^{p} and γ_{sp}^{d} represent respectively the polar and dispersive components of the interfacial energy between proteins and materials), indicating stronger adhesion of albumin than on other P_xC samples and LTIC. The $\gamma_{sp}^{p}/\gamma_{sp}^{d}$ ratio for fibrinogen determined from sample b is 0.04 and which is also small. However, the total interfacial energy γ_{sp} of 6.7 is less than that of albumin, which means less conformational changes. These are believed to be the primary reasons for the good compatibility observed on sample b in our platelet adhesion test.[10]

Consideration must also be given to the blood-biomaterials interface. Because the cellular elements are compatible with blood and they should mechanically stabilize the interface with the medium, the magnitude of the blood-biomaterials interfacial tension is similar to that of the cell-medium interface.[20] The high interface stabilization will provide a foreign surface with a long-term mechanically stable interface with blood. Table 6 shows the results of the contact angles and calculated interfacial energies (γ_{sw}) between water and the materials. All the P_xC samples show more enhanced hydrophilic behavior (38.8°–65°) than LTIC (74.9°) and undoped DLC (68.4°). Sample b also has the lowest value of

Table 4
Interfacial energies between materials and plasma proteins.

Biological	P-C (a)		P-C (b)		P-C (c)		P-C (d)		LTIC		DLC	
substance	γ_{sp}	$\gamma_{sp}^p/\gamma_{sp}^d$	γ_{sp}	$\gamma_{sp}^p/\gamma_{sp}^d$	γ_{sp}	$\gamma_{sp}^p/\gamma_{sp}^d$	γ_{sp}	$\gamma_{sp}^p/\gamma_{sp}^d$	γ_{sp}	$\gamma_{sp}^p/\gamma_{sp}^d$	γ_{sp}	$\gamma_{sp}^p/\gamma_{sp}^d$
Fibrinogen	9.6	0.18	6.7	0.04	12.6	0.24	3.9	1.44	16.8	12.2	9.1	2.2×10^1
Albumin	15.2	0.26	11.1	0.11	19.1	0.30	4.5	0.26	11.8	46.6	5.8	1.4×10^6

Table 5
Ratios of interfacial energies of albumin / fibrinogen γ_{sp} (alb/ fib).

Material	γ_{sp} (alb/ fib)
Sample a	1.58
Sample b	1.66
Sample c	1.52
Sample d	1.15
LTIC	0.70
Undoped DLC	0.63

Table 6
Contact angle (θ_w) and interfacial energy (γ_{sw}) between different materials (samples) and water.

Material	θ_w (°)	γ_{sw} (mJ/m^2)
Sample a	40.6	6.6
Sample b	49.0	5.1
Sample c	38.8	8.9
Sample d	65.0	6.3
LTIC	74.9	24.2
DLC	68.4	16.1

interfacial energy (γ_{sw} = 5.1) with water (medium), which means that this sample has a similar interfacial tension (1–3 mJ/m^2) as the cell-medium interface.

4. Conclusion

Phosphorus-doped carbon (P_xC) films with different phosphorus concentrations are fabricated by plasma immersion ion implantation and deposition (PIII&D) to investigate the relationship between the dopant concentration, surface energy and hemocompatibility of the materials. The films are characterized by XPS, SEM-EDS, TEM, and contact angle tests, and *in vitro* platelet adhesion tests are conducted to estimate the blood compatibility. Our investigation shows that the strongest adhesion of albumin with least conformational change in fibrinogen occurs on the sample with a P to C ratio of 0.27. The sample also has the lowest value of interfacial energy (γ_{sw} = 5.1) with water, which is close to the interfacial tension of the cell-medium interface (1–3 mJ/m^2), thereby providing a more mechanically stable interface. The results reported here serve to explain the observations reported in our previous paper.[10]

Acknowledgments

This research was jointly and financially supported by Hong Kong Research Grants Council (RGC) Competitive Earmarked Research Grant (CERG) #CityU 1120/04E, RGC-NSFC Joint Research Grant N_CityU 101/03, Natural Science Foundation of China (50203001), and Southwest Jiaotong University Foundation (2002B02).

References

1) G. C. Thorwarth, M. Kuhn, W. Assmannc, B. Schey and B. Stritzker: Surf. Coat. Technol. **193** (2005) 206.
2) W. Fortunato, A. J. Chiquito, J. C. Galzerani and J. R. Moro: Thin Solid Films **476** (2005) 246.
3) O. S. Panwar, S. K. Gupta, M. Alim Khan, B. S. Satyanarayana and R. Bhattacharyya: Diamond Relat. Mater. **13** (2005) 513.
4) O. S. Panwara, B. Deb, B. S. Satyanarayanac, M. Alim Khana, R. Bhattacharyyaa and A. K. Palb: Thin Solid Films **472** (2005) 180.
5) K. Yamamoto, H. Watanabe and M. Ogura: Diamond Relat. Mater. **14** (2005) 389.
6) S. R. J. Pearce, J. Filik, P. W. May, R. K. Wild, K. R. Hallam and P. J. Heard: Diamond Relat. Mater. **12** (2003) 979.
7) H. E. Mohammad S. Mominuzzaman, T. Soga, T. Jimbo and M. Umeno: Diamond Relat. Mater. **10** (2001) 984.
8) H. Kato, W. Futako, S. Yamasaki and H. Okushi: Diamond Relat. Mater. **14** (2004) 340.
9) R. Hauert: Diamond Relat. Mater. **12** (2003) 583.
10) S. C. H. Kwok, J. Wang and P. K. Chu: Diamond Relat. Mater. **14** (2004) 78.
11) P. K. Chu: J. Vac. Sci. Technol. B **22** (2004) 289.
12) T. Young: Philos. Trans. R. Soc. London, Ser. 95 (1805) 65.
13) C. J. Van Oss, M. K. Chaudhury and R. J. Good: J Chem. Rev. **88** (1988) 92.
14) M. I. Jones, I. R. McColl, D. M. Grant, K. G. Parker and T. L. Parke: J. Biomed. Mater. Res. **52** (2000) 413.
15) J. H. Elam and H. Nygren: Biomaterials **13** (1992) 3.
16) W. Marconi, A. Galloppa, A. Martinelli and A. Piozzi: Biomaterials **16** (**1995**) 449.
17) T. Y. Liu, W. C. Lin, L. Y. Huang, S. Y. Chen and M. C. Yang: Biomaterials **26** (2005) 1437.
18) P. Yang, N. Huang, Y. X. Leng, J. Y. Chen, R. K. Y. Fu, S. C. H. Kwok, Y. Leng and P. K. Chu: Biomaterials **24** (2003) 2821.
19) C. P. Sharma: J. Colloid Interface Sci. **97**(1984) 585.
20) E. Ruckenstern and S. V. Gourisankar: J. Colloid Interface Sci. **101** (1984) 436.